

Chiral phase transition at finite temperature and conformal dynamics in large N_f QCD

Kohtaroh Miura^a, Maria Paola Lombardo^{a,b}, Elisabetta Pallante^c

^aINFN Laboratori Nazionali di Frascati, I-00044, Frascati (RM), Italy

^bHumboldt-Universität zu Berlin, Institut für Physik, D-12489 Berlin, Germany

^cCentre for Theoretical Physics, University of Groningen, 9747 AG, Netherlands

Abstract

We investigate the chiral phase transition at finite temperature (T) in colour $SU(N_c = 3)$ Quantum Chromodynamics (QCD) with six species of fermions ($N_f = 6$) in the fundamental representation by using lattice QCD with improved staggered fermions. By considering lattices with several temporal extensions N_t , we observe asymptotic scaling for $N_t > 4$. We then extract the dimensionless ratio T_c/Λ_L ($\Lambda_L =$ Lattice Lambda-parameter) for $N_f = 6$ and $N_f = 8$, the latter relying on our earlier results. Further, we collect the critical couplings β_L^c for the chiral phase transition at $N_f = 0$ (quenched), and $N_f = 4$ at a fixed $N_t = 6$. The results are consistent with enhanced fermionic screening at larger N_f . The T_c/Λ_L depends very mildly on N_f in the $N_f = 0 - 4$ region, starts increasing at $N_f = 6$, and becomes significantly larger at $N_f = 8$, close to the edge of the conformal window. We discuss interpretations of these results as well as their possible interrelation with preconformal dynamics in the light of a functional renormalization group analysis.

Keywords: Lattice Gauge Theory, Conformal Symmetry, Chiral Symmetry, Finite Temperature

INTRODUCTION Conformal invariance is anticipated to emerge in asymptotically free non-Abelian gauge theories when the number of flavours exceeds a critical value $N_f = N_f^c$. The approach to conformality for $N_f \lesssim N_f^c$, close to the edge of the conformal window, is in principle associated with a walking behaviour of the running coupling, which has been advocated as a basis for strongly interacting mechanisms of electroweak symmetry breaking.

Recent lattice studies[1] focused on the computation of N_f^c and the analysis of the conformal window itself, either with fundamental fermions [2, 3, 4, 5, 6, 7, 8, 9] or other representations [10, 11, 12, 13]. Among the many interesting results with fundamental fermions, we single out the observation that QCD with three colours and eight flavours is still in the hadronic phase [3, 4], while $N_f = 12$ seems to be close to the critical number of flavours, with some groups favouring conformality [2, 3, 5, 6], and others chiral symmetry breaking [8].

In comparison, much less effort has been devoted to the analysis of the phenomenologically relevant subcritical region [14, 15, 16, 17]. Here, we would like to learn where and how QCD at the edge of the conformal window displays walking, and its associated manifestations like separation of scales and approximate scale invariance. This Letter is one step in this direction.

Building on the above mentioned results, we decided to concentrate ourselves on $N_f \leq 8$, so to be safely in the hadronic region, but not too far from the edge of the conformal window. A recent study [14] noted an enhancement of the zero temperature ratio $\langle \bar{\psi}\psi \rangle / F^3$, where F is the pseudoscalar decay constant. This suggests that $N_f = 6$ might indeed be the onset of new

strong dynamics.

In this letter we study the thermal transition of QCD with $N_f = 0, 4, 6$, and combine our findings with those of our early work for $N_f = 8$ [4]. We confirm the expected enhanced screening when the number of flavours increases, and discuss the interrelation of our results with a possible emergence of a new, preconformal dynamics.

As a general remark, we note that using the thermal transition as a tool for investigating preconformal dynamics was largely inspired by a renormalization group analysis [18], as we will review below. Further reasons of interest for finite temperature studies of large N_f include a connection between the quark-gluon plasma phase and the cold conformal region, which might lend support to analyses of quark-gluon plasma based on the AdS/CFT correspondence.

BRIEF OVERVIEW OF ANALYTIC RESULTS A second zero of the two-loop beta-function of a non-Abelian gauge theory implies, at least perturbatively, the appearance of an infrared fixed point (IRFP) and the restoration of conformal symmetry [20, 21]. In colour $SU(3)$ gauge theory with N_f massless fermions in the fundamental representation, the second zero appears for $N_f \gtrsim 8.05$, before the loss of asymptotic freedom (LAF) at $N_f^{\text{LAF}} = 16.5$.

One expects that conformality should emerge when the renormalized coupling at the would be IRFP is not strong enough to break chiral symmetry. This condition provides the lower bound N_f^c of a so called conformal window in N_f . Analytic studies based on the Schwinger-Dyson equation with rainbow resummations [22, 23, 24] or the functional renormalization group method [18] suggest $N_f^c \sim 12$. An all-order pertur-

bative beta-function [25] inspired by the NSVZ beta-function of SQCD [26] has been conjectured, leading to a bound $N_f^c > 8.25$; N_f^c has also been estimated for different fermion representations [27]. In addition to the lower bound of the conformal window, walking dynamics in the preconformal region is another interesting subject in relation to proposed scenarios of walking technicolor. Instanton studies at large N_f [28] claimed a qualitative change of behaviour at $N_f = 6$.

All the above phenomena happen well into the strong coupling regime, rendering a perturbative prediction unreliable and a non-perturbative analysis mandatory. The genuinely non-perturbative lattice formulation of gauge theories is thus a natural candidate for this study.

Recently, the functional renormalization group (FRG) method has been applied to finite T QCD with varying number of flavours, and the critical temperature for the chiral phase transition was obtained as a function of N_f [18]. In this $T - N_f$ phase diagram, the onset of the conformal window has been estimated by locating the vanishing critical temperature.

Most interestingly, the critical exponents associated with the behaviour of the beta function at the IRFP manifest themselves also in the shape of the thermal critical line in the vicinity of the critical number of flavours N_f^c . In more detail, the line is almost linear with N_f for small N_f , and displays a singular behaviour when approaching N_f^c . As emphasised by the authors in Ref. [18], the result clearly elucidates the universality of the critical behaviour at zero and non-zero temperature in the vicinity of N_f^c . It thus seems a promising direction to extend the knowledge of finite T lattice QCD to the larger N_f region, by using the FRG results as analytic guidance.

In this work we investigate the thermal chiral phase transition for $N_f = 6$ colour $SU(N_c = 3)$ QCD by using lattice QCD Monte Carlo simulations with staggered fermions. $N_f = 6$ is expected to be in the important regime as suggested by the results in Refs. [2, 28]. This work is the first study of $N_f = 6$ staggered fermions at finite T , and it provides an important ingredient to a broader project that studies the emergence of the conformal window in the $T - N_f$ phase diagram. In addition to $N_f = 6$, we compute the critical coupling for $N_f = 0$ (quenched) and $N_f = 4$ at $N_t = 6$, and use the results from Ref. [4] for $N_f = 8$.

SETUP Simulations have been performed by utilising the publicly available MILC code [29]. The setup explained below is the same as the one used for $N_f = 8$ in Ref. [4]. We use an improved version of the staggered action, the Asqtad action, with a one-loop Symanzik [30, 31] and tadpole [33] improved gauge action,

$$S = -\frac{N_f}{4} \text{Tr} \log M[am, U, u_0] + \sum_{i=p,r,pg} \beta_i (g_L^2) \text{Re}[1 - U_{C_i}], \quad (1)$$

where g_L is the lattice bare coupling, and β_i are defined as

$$(\beta_p, \beta_r, \beta_{pg}) = \left(\frac{10}{g_L^2}, -\frac{\beta_p(1 - 0.4805\alpha_s)}{20u_0^2}, -\frac{\beta_p}{u_0^2} 0.03325\alpha_s \right) \quad (2)$$

$$\alpha_s = -4 \log \frac{u_0}{3.0684}, \quad u_0 = \langle U_{C_p} \rangle^{1/4}. \quad (3)$$

The plaquette coupling $\beta_p = 10/g_L^2 \equiv \beta_L$ is a simulation input. The $M[am, U, u_0]$ in Eq. (1) denotes the matrix for a single flavour Asqtad fermion with bare lattice mass am , and U_{C_i} represents the trace of the ordered product of link variables along C_i , for the 1×1 plaquettes ($i = p$), the 1×2 and 2×1 rectangles ($i = r$), and the $1 \times 1 \times 1$ parallelograms ($i = pg$), respectively - all divided by the number of colours. The tadpole factor u_0 is determined by performing zero temperature simulations on the 12^4 lattice, and used as an input for finite temperature simulations.

To generate configurations with mass degenerate dynamical flavours, we have used the rational hybrid Monte Carlo algorithm (RHMC) [32], which allows to simulate an arbitrary number of flavours through varying the number of pseudo-fermions. Simulations for $N_f = 6$ have been performed by using two pseudo-fermions, and subsets of trajectories for the chiral condensates and Polyakov loop have been compared with those obtained by using three pseudo-fermions with the same Monte Carlo time step $d\tau$ and total time length τ of a single trajectory. We have observed very good agreement between the two cases for both evolution and thermalization. We have monitored the Metropolis acceptance and reject ratio, and adjusted $\tau = 0.2 - 0.24$ and $d\tau = 0.008 - 0.016$ to realize the best performance.

Measured observables are the expectation values of the chiral condensate and Polyakov loop,

$$a^3 \langle \bar{\psi}\psi \rangle = \frac{N_f}{4N_s^3 N_t} \langle \text{Tr}[M^{-1}] \rangle, \quad (4)$$

$$L = \frac{1}{N_c N_s^3} \sum_{\mathbf{x}} \text{Re} \left\langle \text{tr}_c \left[\prod_{t=1}^{N_t} U_{4,t\mathbf{x}} \right] \right\rangle, \quad (5)$$

where N_s (N_t) represents the number of lattice sites in the spatial (temporal) direction, $U_{4,t\mathbf{x}}$ is the temporal link variable, and tr_c denotes the trace in colour space. The temperature T is related to the inverse of the lattice temporal extension,

$$T \equiv \frac{1}{a(\beta_L) \cdot N_t}, \quad (6)$$

and we measure $\langle \bar{\psi}\psi \rangle$ and L at various temperatures. The output of this measurement is the critical coupling β_L^c for the chiral phase transition.

RESULTS All results have been obtained for a fermion bare lattice mass $am = 0.02$. In Figs. 1 and 2, the expectation values of the chiral condensate $a^3 \langle \bar{\psi}\psi \rangle$ and the Polyakov loop L are displayed as a function of β_L for several N_t , respectively. It is found that different N_t give a different behaviour of $a^3 \langle \bar{\psi}\psi \rangle$ and L . In particular, this indicates that their rapid crossover with increasing β_L is not to be attributed to a bulk transition. The asymptotic scaling analysis below will confirm that it corresponds instead to a thermal chiral phase transition (or crossover) in the continuum limit.¹

¹For $N_f \geq 3$ we expect a first order chiral transition in the chiral limit, which persists for small values of the quark mass, and ends with a critical endpoint. For larger masses, the transition becomes a crossover. Discriminating among these different behaviours is beyond the scope of this first study.

For $N_t = 4$, it is possible to extract $\beta_L^c = 4.65(25)$ from the peak position of the first derivatives $-a^3 d\langle\bar{\psi}\psi\rangle/d\beta_L$ and $dL/d\beta_L$. For $N_t = 6$, we find a small jump between $\beta_L = 5.0$ and 5.05 , where the Polyakov loop also shows a significant enhancement; hence we estimate $\beta_L^c = 5.025(25)$ for $N_t = 6$. For larger N_t , the signal for the chiral phase transition becomes less clear, and a more refined estimate of β_L^c is necessary. For $N_t = 8$, the Polyakov loop L shows a clear signal as indicated in Fig. 3. In particular, we observe a drastic increase of the Polyakov loop L around $5.2 < \beta_L < 5.3$. The histogram of the chiral condensate around the rapid increase of the Polyakov loop is shown in Fig. 4. At $\beta_L = 5.2$, the histogram exhibits the double-peak structure that indicates the competition between chirally symmetric and broken vacua. Hence, the critical coupling can be estimated as $\beta_L^c = 5.225(25)$ for $N_t = 8$. For $N_t = 12$, we also observe the double-peak structure in the histogram of the chiral condensate around $\beta_L = 5.45$, as shown in Fig. 5, along with the enhancement of the Polyakov loop. All values of the critical lattice coupling β_L^c are summarized in Table 1.

These results can be analyzed and interpreted in terms of the two-loop asymptotic scaling law. Let us consider the two-loop lattice beta function,

$$\beta(g) = -(b_0 g^3 + b_1 g^5), \quad (7)$$

$$b_0 = \frac{1}{(4\pi)^2} \left(\frac{11C_2[G]}{3} - \frac{4T[F]N_f}{3} \right), \quad (8)$$

$$b_1 = \frac{1}{(4\pi)^4} \left(\frac{34(C_2[G])^2}{3} - \left(\frac{20C_2[G]}{3} + 4C_2[F] \right) T[F]N_f \right), \quad (9)$$

for fundamental fermions in $SU(N_c)$ ($C_2[G]$, $C_2[F]$, $T[F]$) = $(N_c, (N_c^2 - 1)/(2N_c), 1/2)$. From Eq. (7) we obtain the well known two-loop asymptotic scaling,

$$\Lambda_L a(\beta_L) = \left(\frac{2N_c b_0}{\beta_L} \right)^{-b_1/(2b_0^2)} \exp\left[\frac{-\beta_L}{4N_c b_0} \right]. \quad (10)$$

Here Λ_L is the so called lattice Lambda-parameter, and $\beta_L = 2N_c/g^2$, with $g = \sqrt{2N_c/10} \cdot g_L$. This definition effectively takes into account the improvement of the staggered lattice action when comparing to the asymptotic scaling law, see Ref. [4]. The equation (6) can be written as

$$\frac{1}{N_t} = \frac{T_c}{\Lambda_L} \times (\Lambda_L a(\beta_L^c)). \quad (11)$$

The left-hand side is a given number, and we have obtained the corresponding β_L^c by lattice simulations. Hence, the quantity T_c/Λ_L on the right-hand side of Eq. (11) can be extracted, and must be unique as long as the asymptotic scaling law Eq. (10) is verified for a given β_L^c .

In Fig. 6, we show the $N_t^{-1} - \Lambda_L a(\beta_L^c)$ plot. The slope of the line connecting the origin and the data points corresponds to T_c/Λ_L . The $N_t = 6, 8$, and 12 points have a common slope to a very good approximation, while the $N_t = 4$ result falls on a smaller slope. The latter is interpreted as a scaling violation

effect due to the use of a too small N_t . The existence of a common T_c/Λ_L for $N_t \geq 6$ indicates that the data are consistent with the two-loop asymptotic scaling Eq. (10), confirms the thermal nature of the transition and that $N_f = 6$ is outside the conformal window, as expected from a previous $N_f = 8$ study [4]. A linear fit provides $T_c/\Lambda_L = 1.02(12) \times 10^3$, which can be interpreted as the value in the continuum limit for $N_f = 6$ QCD.

In order to have a more complete overview, we have performed simulations for the theory with $N_f = 0$ (quenched) and $N_f = 4$, only at $N_t = 6$. These theories are of course very well investigated, however we have not found in the literature results for the same action as ours. Table 1 shows a summary of our results for the critical coupling β_L^c of the chiral phase transition at finite temperature for $N_f = 0, 4, 6$, and 8 - the latter from Ref. [4].

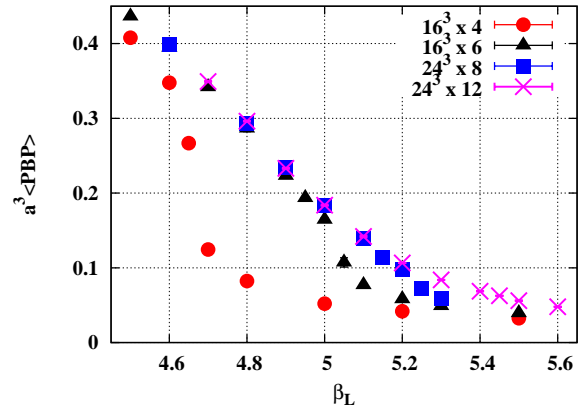


Figure 1: The chiral condensate $a^3\langle\bar{\psi}\psi\rangle$ for $N_f = 6$ and $am = 0.02$ in lattice units, as a function of β_L , for $N_t = 4, 6, 8$, and 12 . Error-bars are smaller than symbols.

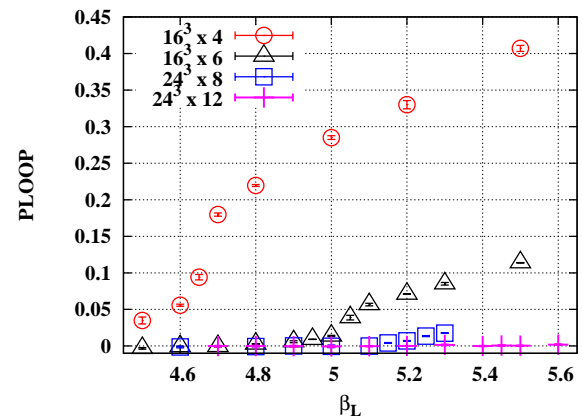


Figure 2: The Polyakov loop L for $N_f = 6$ and $am = 0.02$ in lattice units, as a function of β_L , for $N_t = 4, 6, 8$, and 12 . Error-bars are smaller than symbols.

DISCUSSION In Fig. 7, we display the critical values of the lattice coupling $g_c = \sqrt{2N_c/\beta_L^c}$ from Table 1 in the Miransky-Yamawaki phase diagram.

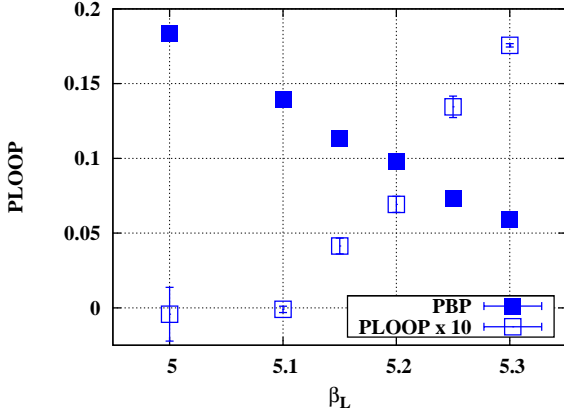


Figure 3: Zoom-in of the chiral condensate $a^3\langle\bar{\psi}\psi\rangle$ and the Polyakov loop L shown in Figs. 1 and 2 in the critical region at $N_t = 8$, with spatial volume 24^3 .

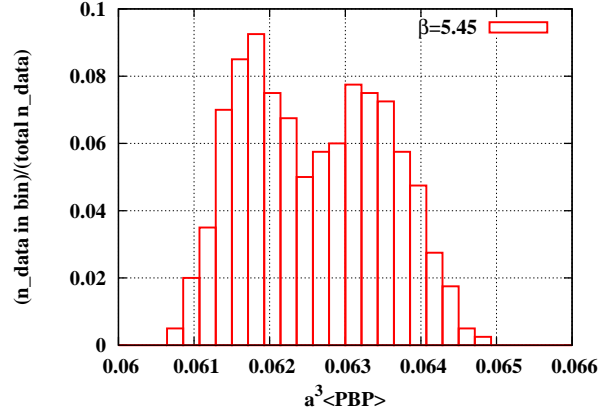


Figure 5: Distribution of the chiral condensate $a^3\langle\bar{\psi}\psi\rangle$ for $N_f = 6$, $am = 0.02$ and spatial volume 24^3 , around the chiral phase transition at $N_t = 12$.

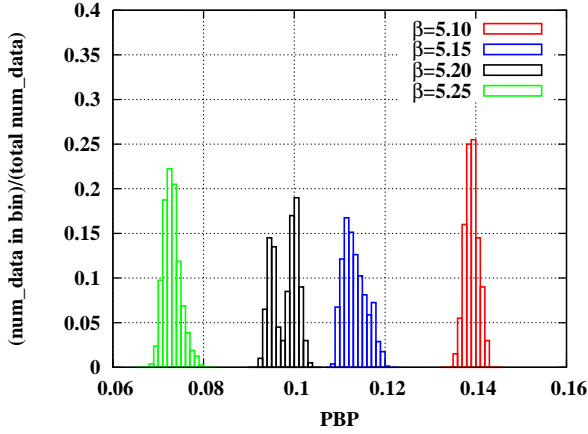


Figure 4: Distribution of the chiral condensate $a^3\langle\bar{\psi}\psi\rangle$ for $N_f = 6$, $am = 0.02$ and spatial volume 24^3 , around the chiral phase transition at $N_t = 8$.

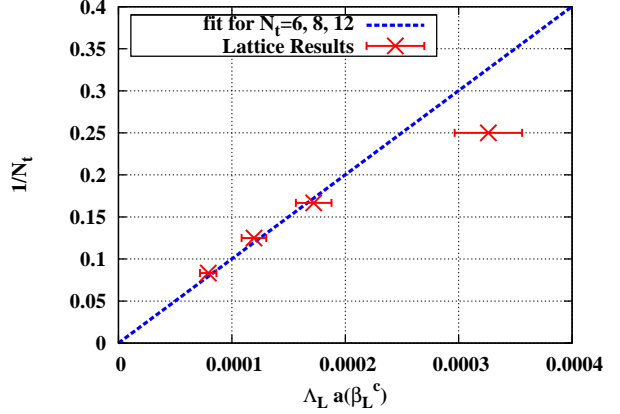


Figure 6: The thermal scaling behaviour of the critical lattice coupling β_L^c . Data points for $\Lambda_L a(\beta_L^c)$ at a given $1/N_t$ are obtained by using β_L^c from Table 1 as input for extracting $\Lambda_L a(\beta_L^c)$ in the two-loop expression Eq. (10). The dashed line is a linear fit with zero intercept to the data with $N_t > 4$.

Consider the $N_t = 6$ results: it is expected that an increasing number of flavours favors chiral symmetry restoration. Indeed, we find that, on a fixed lattice, the critical coupling increases with N_f in agreement with early studies and naive reasoning. The precise dependence of the critical coupling on N_f at fixed N_t is not known. It is, however, amusing to note that the results seem to be smoothly connected by an almost straight line: the brown line in the plot is a linear fit to the data. Comparing the trend for $N_f = 6$ to the one for $N_f = 8$, for varying N_t one can infer a decreasing in magnitude (and small) step scaling function, hence a walking behaviour. Further study is needed at larger N_f , and by using the same action used for $N_f = 0 - 8$, to confirm or disprove it.

Next, we study the N_f dependence of the ratio T_c/Λ_L and related quantities. We recall that the simulations for $N_f = 4$ and $N_f = 0$ have been performed by using only $N_t = 6$. Hence, in these two cases the results will hold true barring strong scaling violations at $N_t = 6$. We note that in a previous lattice study with improved staggered fermions [34], asymptotic scaling was indeed observed for $N_t \geq 6$ for $0 \leq N_f \leq 4$.

Ideally, we would like to convert our results to T_c/Λ_{MS} . Unfortunately, to our knowledge, the conversion from Λ_L to Λ_{MS} for a generic number of flavours is only available for Wilson fermions [35].

Here we consider a simplified procedure, aiming at capturing at least the basic features induced by setting a UV scale. For this purpose, we introduce a reference coupling β_L^{ref} and an associated reference energy scale Λ_{ref} . Then Eq. (10) is generalized as

$$\Lambda_{\text{ref}}(\beta_L^{\text{ref}}) a(\beta_L) = \left(\frac{b_1}{b_0^2} \frac{\beta_L + 2N_c b_1/b_0}{\beta_L^{\text{ref}} + 2N_c b_1/b_0} \right)^{b_1/(2b_0^2)} \exp \left[-\frac{\beta_L - \beta_L^{\text{ref}}}{4N_c b_0} \right]. \quad (12)$$

At leading order of perturbation theory $b_1 \rightarrow 0$, Λ_L and Λ_{ref} are related via

$$\frac{\Lambda_{\text{ref}}}{\Lambda_L} = \exp \left[\frac{\beta_L^{\text{ref}}}{4N_c b_0} \right]. \quad (13)$$

Table 1: Summary of the critical lattice couplings β_L^c for the theories with $N_f = 0, 4, 6, 8$, $am = 0.02$ and varying $N_t = 4, 6, 8, 12$. All results are obtained using the same lattice action.

$N_f \backslash N_t$	4	6	8	12
0	-	7.88 ± 0.05	-	-
4	-	5.89 ± 0.03	-	-
6	4.675 ± 0.025	5.025 ± 0.025	5.225 ± 0.025	5.45 ± 0.05
8	-	4.1125 ± 0.0125	-	4.34 ± 0.04

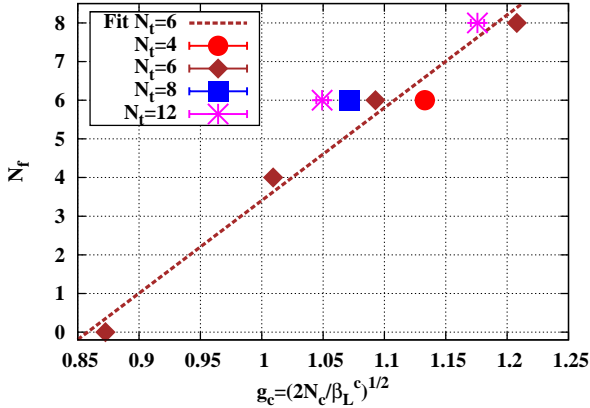


Figure 7: Critical values of the lattice coupling $g_c = \sqrt{2N_c/\beta_L^c}$ for theories with $N_f = 0, 4, 6, 8$ and for several values of N_t in the Miransky-Yamawaki phase diagram. The dashed (brown) line is a linear fit to the $N_t = 6$ results.

This equation would be analogous of the ratio Λ_L/Λ_{MS} derived in [35] for Wilson fermions up to a further linear dependence on N_f in the numerator of the exponent. In a nutshell, the difference originates from the fact that we are fixing a bare reference coupling β_L^{ref} , which will be specified later. Notice that by construction Λ_{ref} reproduces the lattice Lambda-parameter Λ_L in the limit

$$\Lambda_{\text{ref}}(\beta_L^{\text{ref}} \rightarrow 0) = \Lambda_L(1 + \mathcal{O}(1/\beta_L^c)). \quad (14)$$

In summary, when trading Λ_L for Λ_{ref} , we are moving towards a more UV scale.

Let us consider first T_c/Λ_L . The values of T_c/Λ_L are summarized in Table 2, and plotted in Fig. 8. The ratio does not show a significant N_f dependence in the region $0 \leq N_f \leq 4$, it starts increasing at $N_f = 6$, and undergoes a rapid rise around $N_f = 8$. The chiral phase transition would happen when T becomes comparable to a typical energy scale $M_\chi = C\Lambda_L$. The nearly constant nature of T_c/Λ_L in the region $N_f \leq 4$ indicates that the role of such energy scale is not significantly changed by the variation of N_f (see [36] for a detailed discussion of this point.) In turn, the increase of T_c/Λ_L in the region $N_f \geq 6$ might well imply that the chiral dynamics becomes different from the one for $N_f \leq 4$. Indeed, a recent lattice study [14] indicates that $N_f = 6$ is close to the threshold for preconformal dynamics.

We now consider T_c/Λ_{ref} . The N_f dependence of the ratio $R(N_f) \equiv (T_c/\Lambda_{\text{ref}})(N_f)$ is shown for several β_L^{ref} in Fig. 9, where

the vertical axis is normalized by $R(0) = (T_c/\Lambda_{\text{ref}})(N_f = 0)$ for each β_L^{ref} . T_c/Λ_{ref} is now a decreasing function of N_f for a larger β_L^{ref} , *i.e.* for a more UV reference scale Λ_{ref} . This result is consistent with the FRG study [18], where the decreasing $T_c(N_f)$ has been obtained by using the τ -lepton mass m_τ as a common UV reference scale with a common coupling $\alpha_s(m_\tau)$.

The Λ_{ref} scale associated with a $\beta_L^{\text{ref}} \gg \beta_*$ where β_* is evaluated at the infra-red fixed point should provide a UV scale well-separated from the IR dynamics. If we assume the lower bound of the conformal window to be $N_f^c \simeq 12$, the two-loop beta-function leads to $\beta_* = -2N_c b_1/b_0 \simeq 0.63$. Indeed Fig. 9 shows that the decreasing nature of $(T_c/\Lambda_{\text{ref}})(N_f)$ is still weak at $\beta_L^{\text{ref}} = 1.0$. In the limit $\beta_L^{\text{ref}} \rightarrow 0$, T_c/Λ_{ref} reproduces Fig. 8, and the resultant increasing feature should be attributed to the vanishing of Λ_L due to infra-red dynamics. We also notice that β_L^{ref} must always be smaller than β at the UV cutoff, $\beta_{\text{UV}} = \beta_L^c(N_f)$. As shown in Table 1, the lowest value of the critical coupling is given by $\beta_L^c(N_f = 8, N_t = 6) = 4.1125 \pm 0.0125$, hence we constrain our analyses to $\beta_L^{\text{ref}} \leq 4.0$. In summary, Figs. 8 and 9 together show the effects of shifting the reference scales from the IR to the UV.

With the use of a UV reference scale, we should observe the predicted critical behavior [18]

$$T_c(N_f) = K|N_f - N_f^c|^{-1/\theta}. \quad (15)$$

By choosing the critical exponent θ in the range predicted by FRG: $1.1 < 1/|\theta| < 2.5$, our data are consistent with the values $N_f^c = 9(1)$ for $\beta_L^{\text{ref}} = 4.0$ and $N_f^c = 11(2)$ for $\beta_L^{\text{ref}} = 2$. We plan to extend and refine this analysis in the future, and here we only notice a reasonable qualitative behaviour.

Table 2: T_c/Λ_L for several N_f . Results are obtained by using the same lattice action. The value for $N_f = 8$ is extracted from the analysis in Ref. [4].

N_f	T_c/Λ_L
0	600 ± 34
4	620 ± 28
6	1023 ± 117
8	2098 ± 191

SUMMARY We have investigated the chiral phase transition and its asymptotic scaling for $N_f = 6$ colour $SU(3)$ QCD by using lattice QCD Monte Carlo simulations with improved staggered fermions. This study provides an important ingredient to a broader project that studies the emergence of a conformal

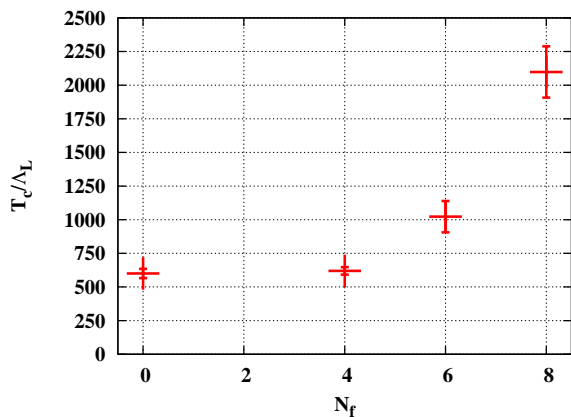


Figure 8: The T_c/Λ_L , for $N_f = 0, 4, 6$ and 8 and lattice bare mass $am = 0.02$.

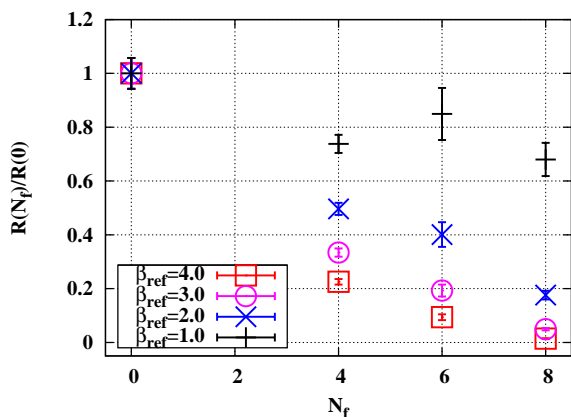


Figure 9: The N_f dependence of $R(N_f)/R(0)$ for several finite fixed β_L^{ref} . Here, $R(N_f) \equiv (T_c/\Lambda_L)(N_f)$. The limit $\beta_L^{\text{ref}} \rightarrow 0$ reproduces the results shown in Fig. 8 up to a renormalization factor and up to a corrections $O(1/\beta_L^c)$.

mal window in the $T - N_f$ phase diagram. We have determined the critical lattice coupling β_L^c for several lattice temporal extensions N_t . We have extracted the dimensionless ratio T_c/Λ_L ($\Lambda_L = \text{Lattice Lambda-parameter}$) for the theory with $N_f = 6$ using two-loop asymptotic scaling. The analogous result for $N_f = 8$ has been extracted from Ref. [4]. T_c/Λ_L for $N_f = 0$ and $N_f = 4$ has been measured at fixed $N_t = 6$, barring asymptotic scaling violations. Then we have discussed the N_f dependence of the ratios T_c/Λ_L and T_c/Λ_{ref} , where Λ_{ref} is a UV reference energy scale, related to Λ_L as in Eq. (13).

We have observed that T_c/Λ_L shows an increase in the region $N_f = 6 - 8$, while it is approximately constant in the region $N_f \leq 4$. We have discussed this qualitative change for $N_f \geq 6$ and a possible relation with a preconformal phase.

The ratio T_c/Λ_{ref} is a decreasing function of N_f . This behaviour is consistent with the result obtained in the functional renormalization group analysis [18], where a common UV reference scale was used to study the chiral phase boundary in the $T - N_f$ phase diagram.

Next steps of the current project involve a scale setting at zero temperature by measuring a common UV observable. It would also be desirable to have the relation between Λ_L and Λ_{MS} for our action. This, together with a more extended set of flavour numbers, will allow a quantitative analysis of the critical behaviour. We expect the resultant $T_c - N_f$ phase diagram to play an essential role in the study of the conformal window.

ACKNOWLEDGMENTS We thank Holger Gies and Jens Braun for fruitful discussions and most useful suggestions. We have enjoyed discussing these topics with Koichi Yamawaki, Masafumi Kurachi, Hiroshi Ohki, Michael Müller-Preussker, Marc Wagner, Biagio Lucini, Volodya Miransky, Albert Deuzeman and Tiago Nunes da Silva. Kohtaroh Miura thanks Michael Müller-Preussker and the theory group in the Humboldt University for their hospitality. Kohtaroh Miura is partially supported by EU I3HP2-WP22. This work was in part based on the MILC Collaboration's public lattice gauge theory code. See <http://www.physics.indiana.edu/~sg/milc.html> for details. The numerical calculations were carried out on the IBM-SP6 at CINECA, Italian-Grid-Infrastructures in Italy, and the Hitachi SR-16000 at YITP, Kyoto University in Japan.

References

- [1] For recent reviews, see L. Del Debbio, PoS **LATTICE2010** (2010) 004; E. Pallante, PoS **LATTICE2009** (2009) 015.
- [2] T. Appelquist, G. T. Fleming, M. F. Lin, E. T. Neil, D. A. Schaich, Phys. Rev. **D84**, 054501 (2011).
- [3] T. Appelquist, G. T. Fleming and E. T. Neil, Phys. Rev. D **79** (2009) 076010; Phys. Rev. Lett. **100** (2008) 171607 [Erratum-ibid. **102** (2009) 149902].
- [4] A. Deuzeman, M. P. Lombardo and E. Pallante, Phys. Lett. B **670** (2008) 41.
- [5] A. Deuzeman, M. P. Lombardo and E. Pallante, Phys. Rev. D **82** (2010) 074503.
- [6] A. Hasenfratz, Phys. Rev. D **82** (2010) 014506.
- [7] A. Hasenfratz, Phys. Rev. D **80** (2009) 034505.
- [8] Z. Fodor, K. Holland, J. Kuti, D. Negradi and C. Schroeder, Phys. Lett. **B703** (2011) 348-358.
- [9] Z. Fodor, K. Holland, J. Kuti, D. Negradi and C. Schroeder, Phys. Lett. B **681** (2009) 353.
- [10] T. Karavirta, A. Mykkanen, J. Rantaharju, K. Rummukainen and K. Tuominen, JHEP **1106** (2011) 061; A. J. Hietanen, K. Rummukainen and K. Tuominen, Phys. Rev. D **80** (2009) 094504; A. J. Hietanen, J. Rantaharju, K. Rummukainen and K. Tuominen, JHEP **0905** (2009) 025.
- [11] Y. Shamir, B. Svetitsky and E. Yurkovsky, Phys. Rev. D **83** (2011) 097502; O. Machtey and B. Svetitsky, Phys. Rev. D **81** (2010) 014501; Y. Shamir, B. Svetitsky and T. DeGrand, Phys. Rev. D **78** (2008) 031502.
- [12] J. B. Kogut and D. K. Sinclair, Phys. Rev. D **81** (2010) 114507.
- [13] Z. Fodor, K. Holland, J. Kuti, D. Negradi and C. Schroeder, JHEP **0911** (2009) 103.
- [14] T. Appelquist *et al.*, Phys. Rev. Lett. **104** (2010) 071601.
- [15] T. Appelquist *et al.* [LSD Collaboration], Phys. Rev. Lett. **106** (2011) 231601.
- [16] S. Catterall, J. Giedt, F. Sannino and J. Schneible, JHEP **0811** (2008) 009; S. Catterall and F. Sannino, Phys. Rev. D **76** (2007) 034504.
- [17] L. Del Debbio, B. Lucini, A. Patella, C. Pica and A. Rago, Phys. Rev. D **82** (2010) 014510; **82** (2010) 014509.
- [18] J. Braun, C. S. Fisher, H. Gies, Phys. Rev. **D84** (2011) 034045; J. Braun and H. Gies, JHEP **1005** (2010) 060; **0606** (2006) 024.
- [19] For a recent review, see F. Sannino, Acta Phys. Polon. B **40** (2009) 3533.
- [20] W. E. Caswell, Phys. Rev. Lett. **33** (1974) 244.
- [21] T. Banks and A. Zaks, Nucl. Phys. B **196** (1982) 189.

- [22] T. Appelquist, J. Terning and L. C. R. Wijewardhana, Phys. Rev. Lett. **77** (1996) 1214; T. Appelquist, A. Ratnaweera, J. Terning and L. C. R. Wijewardhana, Phys. Rev. D **58** (1998) 105017.
- [23] V. A. Miransky and K. Yamawaki, Phys. Rev. D **55** (1997) 5051 [Erratum-ibid. D **56** (1997) 3768].
- [24] T. Appelquist, A. G. Cohen and M. Schmaltz, Phys. Rev. D **60** (1999) 045003.
- [25] T. A. Ryttov and F. Sannino, Phys. Rev. D **78** (2008) 065001.
- [26] V. A. Novikov, M. A. Shifman, A. I. Vainshtein and V. I. Zakharov, Nucl. Phys. B **229**, 381 (1983).
- [27] D. D. Dietrich and F. Sannino, Phys. Rev. D **75** (2007) 085018.
- [28] M. Velkovsky and E. V. Shuryak, Phys. Lett. B **437** (1998) 398.
- [29] MILC Collaboration, <http://www.physics.indiana.edu/~sg/milc.html>
- [30] C. Bernard *et al.*, Phys. Rev. D **75** (2007) 094505.
- [31] M. Luscher and P. Weisz, Phys. Lett. B **158** (1985) 250; Commun. Math. Phys. **97** (1985) 59 [Erratum-ibid. **98** (1985) 433].
- [32] M. A. Clark, PoS **LAT2006** (2006) 004.
- [33] G. P. Lepage, P. B. Mackenzie, Phys. Rev. D **48** (1993) 2250.
- [34] S. Gupta, Phys. Rev. D **64** (2001) 034507.
- [35] H. Kawai, R. Nakayama and K. Seo, Nucl. Phys. B **189** (1981) 40.
- [36] J. Braun, Phys. Rev. **D81** (2010) 016008.